A computational study of CH4 adsorption on Ru-Cu (100) binary alloy surface

Author[1,*], Author[2], Author[3]

Habib KHETTAL, Hiba KHATIR, Mebarek BOUKELKOUL and Mohamed Fahim HAROUN*

Laboratoire de Physique Quantique et Systèmes Dynamiques, Department of Chemistry, Faculty of Sciences, Sétif 1 University- Ferhat ABBAS, 19000 Algeria

* Corresponding author: mohamed.haroun@univ-setif.dz

Abstract

The first principle density functional theory calculations (DFT GGA-PW91) have been used to study the activity of Ru-Cu(100) bimetallic surface for methane adsorption. The study involved the possible and the favorite adsorption sites for methane with different adsorbed configurations at a coverage of 0.25 monolayer. The structural parameters of all adsorbed species are presented. As a result, it is found that the Ru atom stabilizes the adsorption of CH4 better than the other surface sites with a weak chemical interaction.

Classification: Insert here classification codes, separated by a comma

Keywords: DFT, Methane adsorption, binary alloy, Ru-Cu(100) surface, catalytic activity.

1. Introduction

Breaking or forming chemical bonds requires crossing energy reaction barriers and, in the absence of a catalyst, high temperature and pressure conditions are needed. In addition, a chemical reaction usually results in several products. Heterogeneous catalysis is also an important sector of nano-science, by the use of nano-objects such as transition metal-based surfaces to convert fossil or renewable raw materials into synthesis gas and/or hydrogen for which methane is the particularly interesting source. A number of strategies to convert methane are investigated at different levels, ranging from fundamental science research to engineering technology. This includes steam methane reforming (SMR) to produce hydrogen and synthesis gas, followed by Fischer–Tropsch chemistry of which the main reaction consists in the combination of hydrogen and carbon monoxide to produce liquid hydrocarbons and oxygenated hydrocarbons. Besides the complete methane dissociation that transforms CH4 into C and H on catalyst surfaces is used for the production of carbon nanofibers and graphene for device applications.

Indeed, methane is the alkane that has the highest H/C ratio and its dissociation to produce hydrogen is currently the subject of many research works. In fact, this polyatomic molecule is small enough to be processed by a theoretical calculation at very high level [1].

However, the high stability of C-H bond (432 kJ mol−1) [2] in gas phase makes it hard to dissociate at the room temperature and hence, for this purpose, a catalyst remains necessary. In fact, the dissociation of methane using transition metals has been studied by many authors on different mono and bimetallic catalytic surfaces [3-9]. The catalysts used to transform methane are mainly transition metals (TM) including Ni and Cu, precious metals (such

* Corresponding author

as Pt, Pd, Ru and Rh), and transition metals alloyed with precious metals [10-16]. These alloy catalysts based on precious metals were shown to be good candidates for methane activation [17-21].
Several experimental studies have been carried out on the interaction of CHx species with ruthenium-based surfaces. Ahlafi et al.[22] used Ru/Al2O3 as catalyst to make carbon monoxide react with hydrogen. The mass and FTIR spectrometric techniques in separate flow and reactor systems revealed that CxHy species give a peak of methane during hydrogenation. While using temperature programmed desorption (TPD) and high resolution electron energy-loss spectroscopy (HREELS), Wu et al. [23,24] found that the methane dissociation on Ru(0001) and Ru($11\bar{2}0$) leads to the formation of various hydrocarbon intermediates. The apparent activation energy of methane C-H cleavage on Ru(0001) surface is about 0.37 eV. Larsen et al. [25] investigated the reactivity of Co films deposited on Cu(111), they showed that the cobalt deposited on copper (111) surface is more reactive than pure Co for methane dehydrogenation. Two steps are investigated by Koranne et al.[26] to convert methane to higher hydrocarbons on Ru/SiO2 and Cu-Ru/SiO2 catalysts. They noticed that high initial yields of Ru/SiO2catalyst result in a complete activation after a few cycles. For Cu-Ru/SiO2, the methane yield was improved, but the methane conversion decreased with copper content.
Only a few theoretical studies have been devoted to examine methane interaction with ruthenium surfaces. Ciobîca et al.[27] experienced the steps of methane dissociation on Ru(0001) surface by means of DFT periodic calculations. Each transition state of methane decomposition process is analysed. They reported barriers of 0.88 eV for methane decomposition, 0.50 eV for methyl decomposition, and 0.16 eV for methylene decomposition. The corresponding geometry of the first transition state of methane dissociation is very close to that found by Burghgraef et al.[4]. CHx chemisorptions and transition states for C-H activation on the Ru($11\bar{2}0$)surface have been explored by Ciobîca et van Saten [28] using ab- initio periodic DFT calculations. They reported that a bridge-up site of surface Ru ($11\bar{2}0$) stabilizes better all adsorbed species (CHx, X=3-1), while atomic C prefers top-down site. The corresponding barriers for methane complete decomposition CHx → CHx-1 + H are between 0.11 eV and 0.98 eV. Recently Arevalo et al.[29] elucidated the reaction mechanism of methane steam reforming (SMR) onRu($11\bar{2}0$)surface catalyst using first principle calculations that based on DFT. They provided insights about methane activation, which proceeds in a thermodynamically exothermic dissociative adsorption resulting in CHx species.
On the other hand, further focusing on Ru based surfaces, the literature reported that only methane activation on Ru(0001) [27] and Ru($11\bar{2}0$) [28,29] has been investigated and showed an excellent catalytic performance.
Using DFT and the generalized gradient approximation (GGA), Carey et al. [30] investigated the dissociative adsorption of methane on Cu and Zn doped CeO2 (111). They showed that the C-H cleavage occurs locally at the dopant cations, and that Zn-doped CeO2 surface is thermodynamically and kinetically more favorable than Cu-doped CeO2 surface.
He et al. [31] explored the influence of tensile strain on the catalytic properties of Cu(100) surface for CH4 dissociation, exploiting DFT approach and micro kinetic model. They concluded that the strain hinders the methane dissociation process on Cu(100) surface and the methane activation rate is sensitive to the surface constraint.
On the other hand, the activation barriers of the different steps of methane dehydrogenation can be adjusted by doping, adsorbing or alloying the catalyst by metallic impurities. Yuan et al. [32] demonstrated that the adsorption of a single Ni atom on Cu(100) has remarkably improved the catalytic reactivity compared to the flat Cu(100) surface. Otherwise, Kokalj et al. [33] have shown that the combination of very active reaction center (Rh) with inert substrate (Cu(111)) may prevent methyl dehydrogenation. Zhang et al. [34] revealed that the adsorbed or substituted Rh atom on Cu(111) catalyst has remarkably reduced the activation barriers for the complete CH4 dehydrogenation process, which indicates that precious Rh atom on Cu catalyst exhibits better reactivity for CH4activation.
According to these studies, precious metal atoms adsorbed or substituted on inert copper-based surfaces improves its catalytic proprieties. To the best of our knowledge, the bimetallic CuRu(100) surface structure and the methane dissociation on this catalyst surface have no report.
Copper, as one of transition metals, has been widely studied and used for many hydrogenation and dehydrogenation reactions [5, 11, 13, 30-39]. The latter suggest that copper catalysts alloyed to precious metals have a high potential to be used in the process of hydrogen production. In addition, it would appreciably reduce the cost if Cu-based catalysts are developed for these reactions.
Regardless these few theoretical and experimental studies were published about the metals alloyed with Cu catalyst to achieve appreciable catalytic performance for methane activation. Hence, the present work focuses on the effect of copper catalyst doped by ruthenium CuRu(001) surface. This choice is motivated by the experimental data [22-

25,40,41] which showed that the precious metals such as Ru, Rh, Pd and Pt have a high activity for methane activation, particularly ruthenium. On the other hand, it is interesting to explore new cheaper catalysts with high performance. It is important to give insights into the catalytic interaction of CH4 and pathway towards CH3+H formation on Ru-Cu (001) surface. These results would provide significant information on ruthenium and copper-based catalysts and their efficiency for methane dissociation.
In this paper, the reaction of methane is presented using Ru-Cu(001) as catalyst. The first principle calculations are operated using DFT to illustrate how the ruthenium interacts with Ru-Cu(001) surface. Methane adsorbed geometries and electronic structures are also analyzed.

2. Theoretical Method

In this work, all computational calculations are carried out using Dacapo program [42,43] based on ultrasoft pseudo potentials [44] in the framework of the DFT. The Kohn-Sham-one electron valence states are expanded on a plane wave basis set with a cut-off energy extended to 400 eV. For the treatment of the exchange-correlation potential energy, the Perdew-Wang (GGA-PW91) generalized gradient approximation is used [45]. The first Brillouin zone is sampled with The Monkhorst-Pack [46] grid using 5×5×1 k-points mesh. In order to facilitate the convergence, a Fermi broadening corresponding to a k_BT = 0.1 eV is used.

The considered systems are modeled by a five-layers slab. The top most layer corresponding to 75% Cu and 25% Ru with 2×2 unit cell is taken to reduce the interaction between adsorbed compounds. In the other side, a vacuum space of 17 Å is supplied to avoid interaction with adjacent slabs. The adsorbed compounds are located on one face of the slab with a coverage of 0.25 monolayer (ML) to reduce the interaction between the adsorbates. The three top atomic plans and the adsorbate are allowed to relax freely and the two bottom ones are maintained frozen in the bulk position. The force convergence criterion is 0.05 eV/Å, and the adsorption energies are as follows:

$$-E_{ads} = E_{adsorbate/RuCu} - E_{RuCu} - E_{adsorbate}$$

Where $E_{adsorbate/RuCu}$ stands for the total energy of the Ru-Cu(100) slab and adsorbate. E_{RuCu} is the slab energy and $E_{adsorbate}$ is the energy of the isolated adsorbate in the gas phase.

It is worthy to note that the negative sign of Eads ensures the positive adsorption energies to stabilize the surface of the studied systems.

3. Results and Discussion

3.1 Adsorbed CH4

3.1.1 CH4 Adsorption Energies on Ru-Cu(100) Surface

Number figures consecutively and align it's at the middle of the page. Insert figures after they are cited in the text
First, the proprieties of CH4 in gas phase are checked whether they are well reproduced. In fact, the optimization of the CH4 molecule revealed that the C-H bond length is around 1.097 Å and the H-C-H angle value is109.5°, which is in good agreement with the literature [47].
Ru-Cu (100) surface presents three high-symmetry adsorption sites, as displayed in Fig.1.

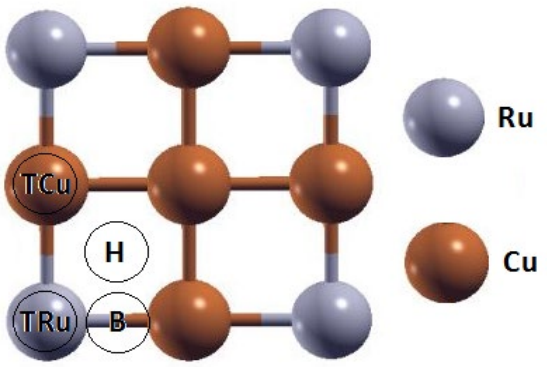

Figure1. Top view of the (2 × 2) Ru-Cu(100) surface with the TRu (Ru top site), TCu (Cu top site),B (bridge site), H (hollow site).

The adsorbed species could be located on Ru or Cu top, bridge or hollow sites, hereafter labeled T (Ru or Cu), B and H respectively. Several orientations of CH4 were considered at each site. The resulting configurations are designated by the site label and the number (1, 2 or 3) of hydrogen atoms oriented to the surface before geometrical optimization, as shown in Fig. 2. In the case of bridge site, only the B3 configuration is stable, while the configurations with one and two hydrogen atoms oriented to the surface are unstable, and the molecule diffuses to the Ru top site.

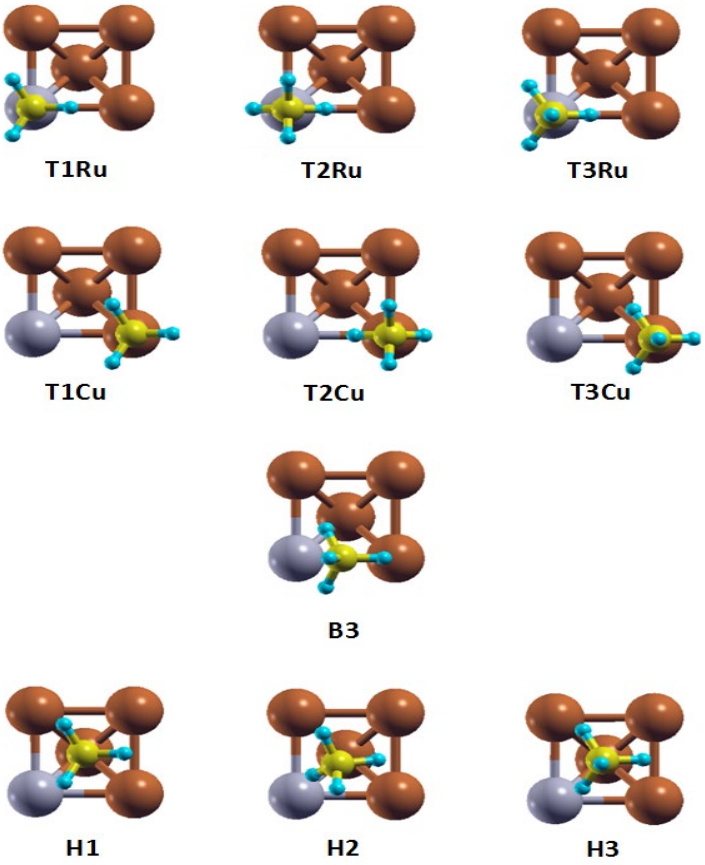

Figure 2. Top view of the TRu, TCu, B, and H configurations of CH4 adsorbed on Ru-Cu(100) after geometrical optimization.

It is to be noted that the symmetry of the molecule before optimization is conserved for all configurations. The calculated energies and structural parameters of methane adsorbed on the various sites with different orientations are summarized in Table 1.

It can be seen from Table 1 that the obtained adsorption energies vary from 0.07 eV to 0.15 eV, for the top configurations. For the hollow and bridge configurations, the interaction of adsorbate with surface ranges between 0.07 eV and 0.08 eV. Note that methane configuration with one and two hydrogens oriented to bridge sites are considered, and found to be unstable.

The above calculations indicate that the interaction of the methane with the metal surface is weak on the Cu top site, and in the hollow site with adsorption energies in physisorption level (0.06-0.08 eV), and a little stronger interaction on Ru top site with energies from 0.13 eV to 0.15 eV. It is clear that for the most stable configurations, the molecule orientation affects weakly the adsorption energy and its variation is in the order of 0.02 eV, which can be considered as a rotation barrier.

Adsorption sites	Eads(eV)	C–H (Å)	C–CuRu (Å)	α1 (deg)	α2 (deg)	α3 (deg)	α4 (deg)	α5 (deg)	α6 (deg)
T1Ru	0.131	1.115	3.14	108.22	108.26	108.26	110.66	110.66	110.66
T2Ru	0.150	1.117	2.71	112.48	111.77	108.55	108.55	107.76	107.76
T3Ru	0.070	1.099	3.39	109.67	109.67	109.71	109.33	109.09	109.33
T1Cu	0.075	1.099	4.15	109.36	109.35	109.36	109.64	109.55	109.55
T2 Cu	0.067	1.098	3.78	108.95	109.86	109.49	109.51	109.50	109.39
T3 Cu	0.073	1.098	3.84	109.29	109.29	109.44	109.60	109.57	109.60
H1	0.074	1.101	3.74	109.16	109.16	109.45	109.76	109.76	109.64
H2	0.082	1.097	3.65	109.06	109.94	109.72	109.66	109.04	109.39
H3	0.070	1.099	3.61	109.16	109.41	109.31	109.41	109.77	109.72
B3	0.076	1.099	3.61	109.24	109.24	109.65	109.43	109.82	109.72

Table 1. Calculated adsorption energies and structural parameters for CH4 adsorbed on CuRu(100) surface sites with different orientations.

The results in Table 1 show clearly a large variation in the adsorbed energies between the configurations. Therefore, the potential governing the interaction of methane with CuRu(100) surface is not flat. The high potential on the Ru top site can justify the diffusion of the methane adsorbed on the bridge site, with one and two hydrogens pointing to the surface, to the Ru top site. These results indicate that CH4 adsorbs preferably on the Ru top site rather than the other surface sites.

Several investigations have been realized on the interaction of methane with transition metal surfaces. It was found that the most of them have very weak adsorption energies. Indeed, Lai et al. [48] calculated by a DFT-slab method, the adsorption energies of methane on the Ni(100) surface with several orientations of the molecule relative to the surface. They found adsorption energy values between 0.05 eV and 0.06 eV. However, when using VASP code, Sorescu [49] found that the adsorption energies of methane on the Fe(100) surface with different configurations is located between 0.017 eV and 0.039 eV. Haroun et al. [50] and Moussounda et al. [16] studied respectively the methane adsorption on Ni(111) and Pt(100) surfaces using DACAPO code. The reported adsorption energies in better cases varied between 53 meV and 59 meV, respectively. They concluded that the interaction of methane with Ni and Pd transition metal surfaces is weak. On the other hand, and according to prior theoretical studies of Li et al. [18], the methane interaction on NiM (M= Pd, Co, Rh, Ir) alloy surfaces was reported to be a physisorption process, with very small adsorption energies (between 0.02 eV and 0.03 eV). Besides, Fan et al.[13] exploring the physical origin of the synergic effect of NiM (M=Cu, Ru, Rh, Pd, Ag, Pt, and Au) surface alloys using CH4 dissociation. It is to be noted that CH4 is predicted to be physisorbed with small adsorption energies of -0.02 eV on all the alloyed surfaces.

The first conclusion to be drawn is that the values obtained in the present work suggest that the methane interacted with surface on the Ru top site. These high relating values may be attributed to the effect of the presence of Ru-Cu alloy. Indeed, the incorporation of Ru into the Cu surface has improved significantly its properties. In order to

explain these two characteristics, which have been well specified before, the geometrical and electronic structures of the adsorbate on this surface are studied.

3.1.2 Geometric Structures of CH4/Ru-Cu (100)

Before starting the discussion in this subsection, it is very important to note that the angles between hydrogen-carbon-hydrogen (H-C-H) for configurations with 1, 2 and 3 hydrogens directed to surface are presented in Fig. 3, and the parameters of B1 and B2 configurations are not depicted in the table 1. The molecules spread to the T1Ru site after the optimization and presented the same structural parameters as the latter.

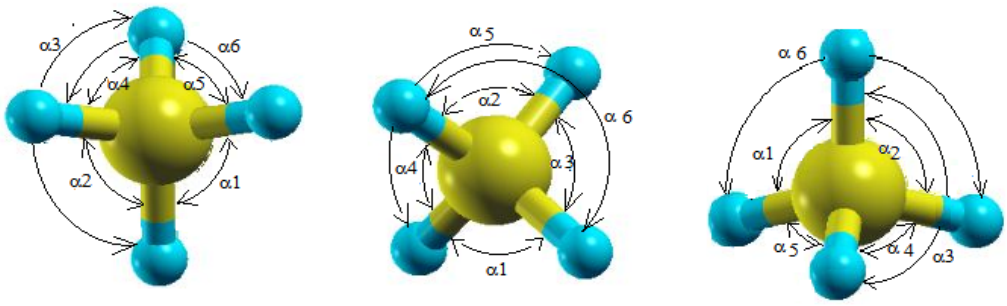

Figure 3. CH_4 angles for different geometric orientations.

Table 1 shows the geometrical parameters of the methane configurations. First, the comparison of the calculated H-C-H angles on these configurations with free methane showed that the interaction tends to reduce the angles between the hydrogen atoms directed to the vacuum and the one pointing towards the surface and to open further the H-C-H angles between the hydrogen atoms directed to the vacuum compared to that calculated (109.5°) in gas phase methane. For T1Ru, T1Cu, H1 configurations, the most open angle reaches the 110.66° value in the T1Ru configuration and the less open reaches the value of 108.22 for the same configuration. To open the two angles towards the surface and towards the vacuum, and then to reduce the angles between H directed towards the vacuum, the carbon and H directed towards the surface. For T2Ru, T2Cu and H2 configurations, the most open angle is 112.48°, and the most closed one reaches the value of 107.76° for the same configuration.

In a second step, we compared the C-H bond lengths in these different configurations. We can distinguish two results: (i) C-H bond lengths of hydrogen directed to vacuum are of the same order of magnitude (1.097 Å) as that of CH4 in the gas phase, (ii) stretching C-H bond length is directed to the surface, reaching successfully the values of 1.117 Å and 1.115 Å for T2Ru and T1Ru configurations respectively.

Similarly, it can be seen that the methane adsorbed on T2Ru site configuration is much more deformed. This result can be explained by the large value of adsorption energy calculated for this configuration. We have also found that the vertical distance between the carbon atom of the molecule and the Z-surface (Carbon-surface) is very short for the configuration T2Ru (2.71Å). One can justify that by the presence of a big wall of potential on this site.

3.2 Projected Density of States of adsorbed CH4 Molecule at T1 Cu top Site

Number equations consecutively within parentheses and align it's at the middle of the page. Insert equations after they are cited in the text like equation (1).
To investigate the electronic properties, we have plotted the sum of s and p projected density of states (PDOS) of adsorbed molecule in the T1Cu configuration compared to the free molecule. The curve of adsorbed molecule in Fig. 4 has two peaks at -4.7 eV and -12.2 eV. These peaks are the combination result of atomic orbitals H(s), C(s) and C(p). The curve is almost similar to those of the free molecule (dashed line) with a small difference.

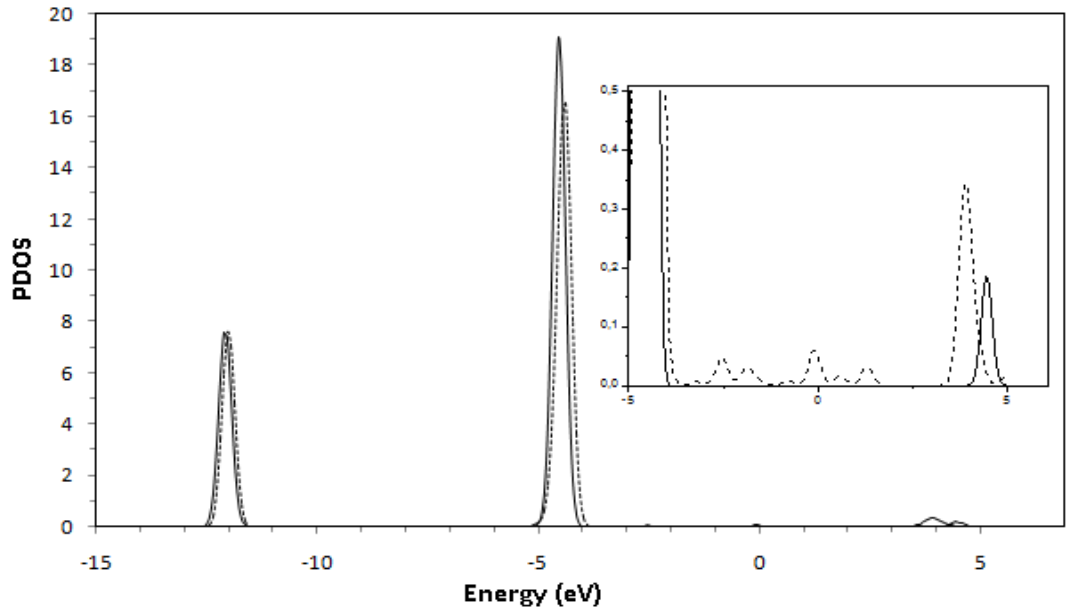

Figure 4. Projected density of state of CH4 molecule adsorbed in the T1Cu configuration (dashed line) and free molecule (full line). The Fermi level is the origin of the energy scale.

It is clear that the peak at -4.7 eV is broadened with an intensity decrease when the molecule is on the surface. We note also some delocalized weak states appearing from -4 eV up to 4 eV which are the contribution of sp carbon states and s states of hydrogen oriented to the surface. The sp, and 3d (not presented here) changes induced by CH4 molecule for the Cu atom of T1Cu configuration are very weak which means that the interaction is very limited and its range is more representative of physical origin. Otherwise, the cooper work function is decreased by $\Delta\varphi = 0.20$ eV, which suggest some polarization due to the adsorbate/surface interaction as mentioned for organic molecules adsorbed on metal surfaces [51]. This means that the dipole is formed, revealed by the work function decreases which is the result of internal polarizations of the molecule and of the surface. This is due to their mutual interaction which induced charge redistribution, indicating a weak van der Waals-type interaction between CH4 and copper metal atom.

Projected density of states of adsorbed CH4 molecule at T2 Ru top site

Among configurations of CH4 adsorbed on the ruthenium, we only analysis the PDOS of the optimal configuration T2Ru. As a consequence of methane interaction with surface, the electronic structures for methane molecule and surface are changed. First, we note that the work function of covered surface is lowered compared to T1Cu configuration. The lowering is $\Delta\varphi = 0.53$ eV showing that the polarization between molecule and surface is now more important than when CH4 is on the top cooper site. Second, the PDOS for adsorbed molecule with T2Ru configuration presented in Fig. 5 shows that the molecular gas peak located at -12.2 eV is shifted by 1.8 eV towards low energies. As this peak is far from 4d Ru band region, we would essentially attribute this shift to the polarization induced by the molecule adsorption. While the peak, at -4.7 eV for free molecule, is shifted and divided after adsorption into two peaks: one at -6.5 eV (β) and the other at -6 eV (α). The two peaks (α) and (β) are shifted by 2 eV and 1.5 eV respectively, compared to that of methane gas phase.

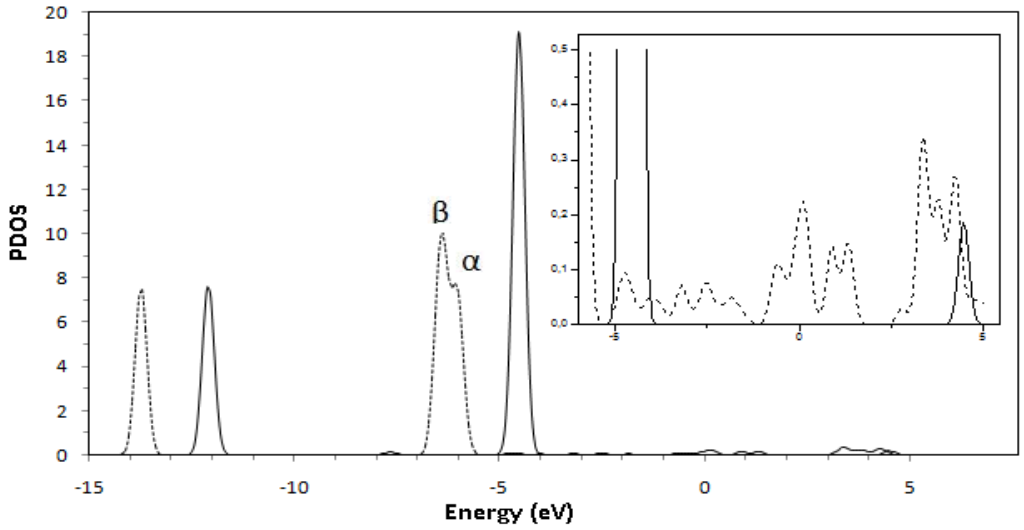

Figure 5. Projected density of state of CH4 molecule adsorbed in the T2Ru configuration (dashed line) and free molecule (full line). The Fermi level is the origin of the energy scale.

Fig. 6 inset shows that the electronic states contributing to (α) peaks are mainly pz orbital of carbon and s of hydrogen directed to the vacuum. Whereas that of (β) peaks are mainly from px, py and pz of carbon and s of hydrogen states oriented to surface. The split in two components (α) and (β) of molecular peack indicating that σ bonding interactions are modified after adsorption. It also means that C sp3 hybridization is partially lifted. Otherwise, as consequence of direct interaction the angles between the carbon and the hydrogens directed towards surface (α1) and vacuum (α2), are opened. This result probably improves the overlap between s(H)-pz(C), s(H)-px(C) and s(H)-py(C).

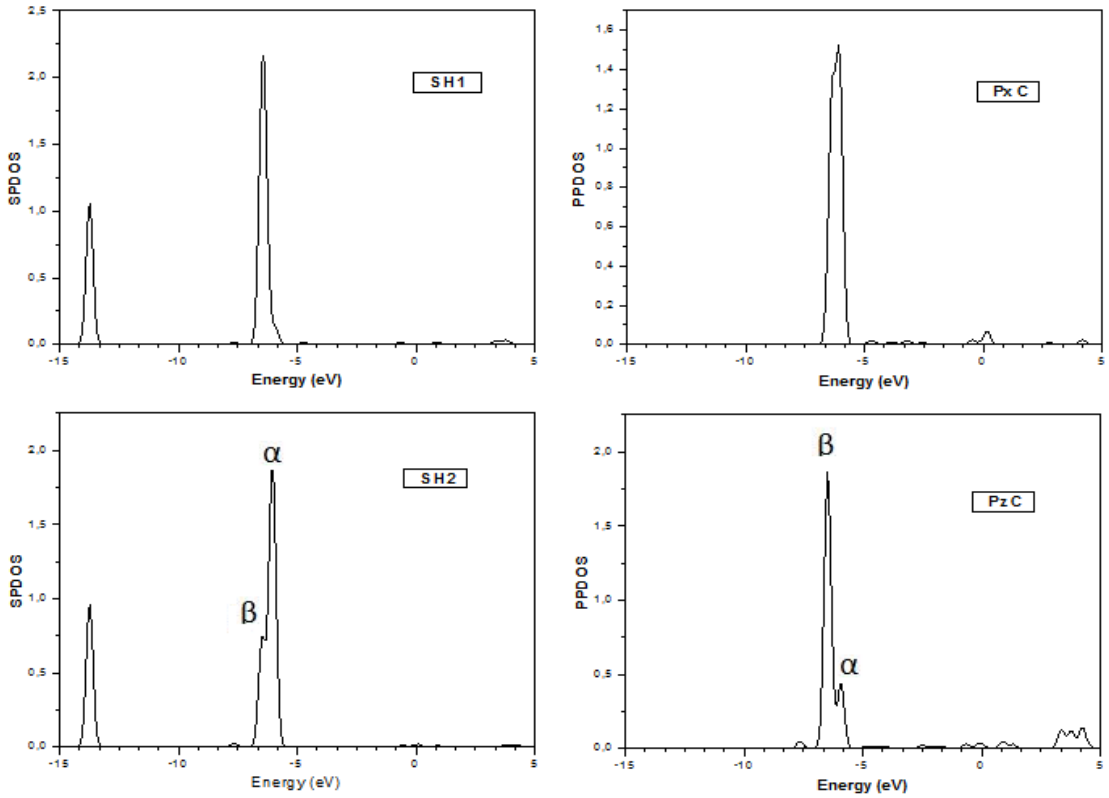

Figure 6. Projected density of state of s H1 (hydrogen towards the surface), s H2 (hydrogen towards the vacuum), px C and pz C.

In addition, it can be seen in Fig. 5, some weak states spread from -5 eV to +5 eV region. The main apparent peaks are around -4.75 eV, -2.5eV, 0.1 eV, 1 eV, 1.25 eV and 3.5 eV. They are mainly C(p) and H(s) states. These states resulting from a faint mixture with Ru states suggesting molecule/surface state transfer.
The Ru sp changes induced by adsorbed CH4 on Ru shown in Fig. 7, calculated as the difference between the respective PDOS after and before methane adsorption. It reveals gain around -6.5 eV and lose at -6 eV in the resonance with the (β) and (α) features detected respectively on the PDOS of adsorbed molecule. The more important peaks resonances are aboveFermi level(FL). These new unoccupied states mean that sp interaction with molecule is mainly non-bonding.

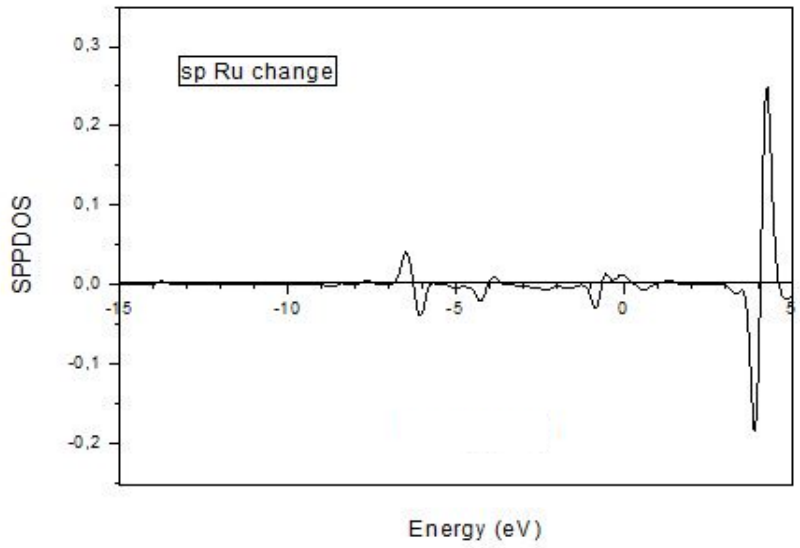

Figure 7. Ru sp projected density of states change upon CH4 adsorption on the CuRu(100) surface with a T2Ru configuration. The Fermi level is the origin of the energy scale.

On the other hand, it can be seen that the induced 4d PDOS states of Ru represented in the Fig. 8 are gained and lost from -7 eV to 5 eV. The curve exhibits peaks which coincide with molecular resonance peacks (α) and (β). Note that new unoccupied states located at 1 eV and 4 eV and the more important gain is around -1 eV. States are lost around FL which signifies that these states are passed to the molecule, showing that this is a channel for ruthenium to molecule back-donation. This means that a weak chemical character is appeared, i.e. states transfer has occurred between surface and molecule involving essentially 4d (Ru) states in one side and p(C) states in the other side, with some contribution s(H) states.

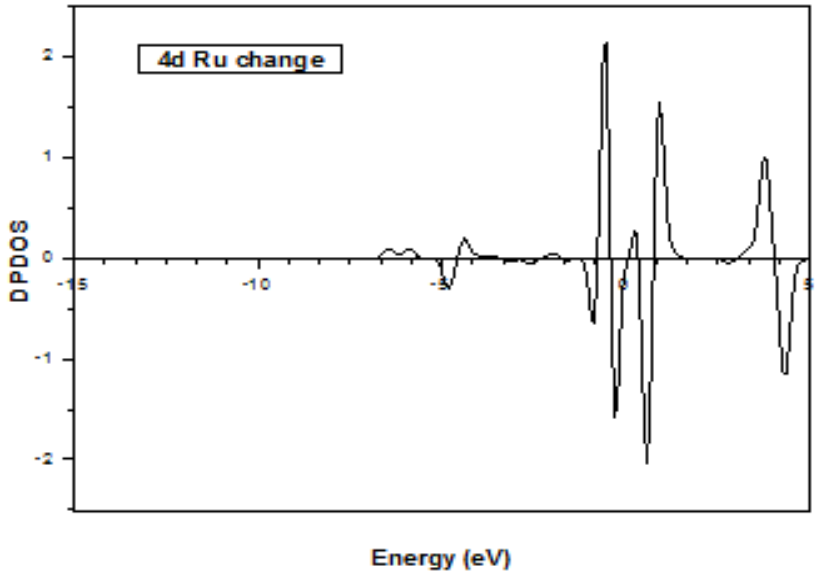

Figure 8. Ru d projected density of states change upon CH4 adsorption on the Ru-Cu(100) surface with a T2Ru configuration. The Fermi level is the origin of the energy scale.

To explain the stability of the molecule adsorbed on the top Ru, we report on Fig. 9, the 4d and 3d projected states densities of Ru and Cu respectively. It is clear that the 4d band of Ru present a high density around FL which is not present on the 3d band of Cu. On the other hand, the d-band center of copper and ruthenium can be considered as a parameter monitoring the surface reactivity. In fact, Hanmmer and Nørskov showed that the catalytic activity and the reactivity of metal system are correlated to the d-band center. They found that the catalytic proprieties increase when the band center is closer to the Fermi level [52,53]. The d-band center of Ru on Ru-Cu(001) surface is closer to FL than Cu.

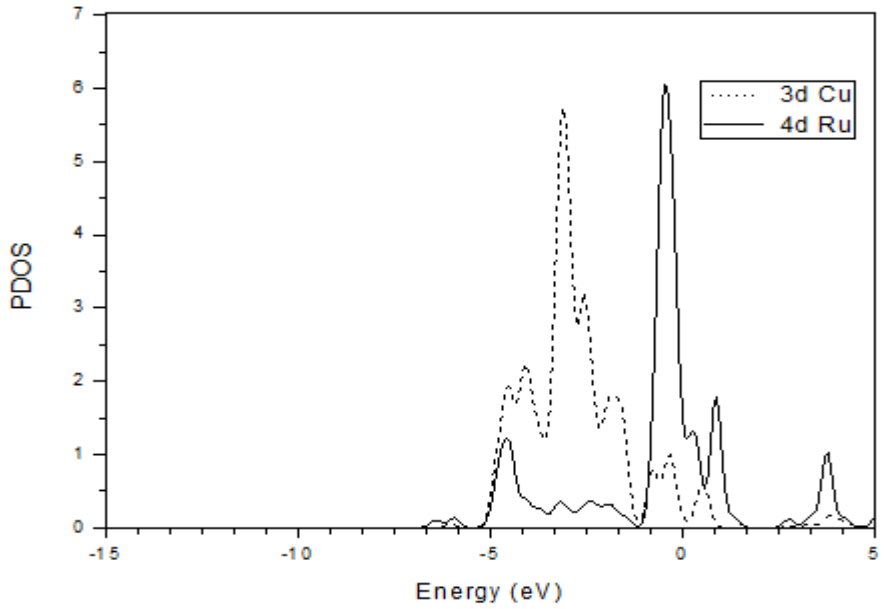

Figure 9. d projected density of states for Cu atom (dashed line) and Ru atom (full line). The Fermi level is the origin of the energy scale.

4. Conclusion

In this paper we used theoretical calculations within the DFT framework to investigate the adsorption of CH4 on Ru-Cu(100). The most stable site of adsorbed methane configurations is identified on the basis of adsorption energies. We found that ruthenium top site is the favored adsorption sites for CH4. We also found from the electronic analysis that methane is weakly chemisorbed on ruthenium top site. These means that the alloyed Ru-Cu(100) surface have a good catalytic performance towards methane dehydrogenation.

References

1. P. M. Hundt, M. E. van Reijzen, H. Ueta, R. D. Beck, J. Phys. Chem. Lett. 5 (2014) 1963-1967.
2. W. M. Haynes, CRC Handbook of Chemistry and Physics, 96th ed., 2015, CRC Press.
3. Q. Qi, X. Wang, L. Chen, B. Li, Appl. Surf. Sci. 284 (2013) 784-791
4. H. Burghgraef, A. P. J. Jansen, R. A. van Santen, Surf. Sci. 344 (1995) 149-158.
5. H.Y. Liu, R.G. Zhang, R.X. Yan, J.R. Li, B.J. Wang, K.C. Xie, Appl. Surf. Sci. 258(2012) 8177-8184.
6. S. Jo, H. D. Son, T.-Y. Kim, J. H. Woo, D. Y. Ryu, J. C. Kim, S. C. Lee, K. L. Gilliard-Abdulaziz, Chem. Eng. J. , 469 (2023) 143772
7. L. Fu, R. Zhang, J. Yang, J. Shi, H.-Y. Jiang, J. Tang, Adv. Energy Mater , 13 (2023) 2301118.
8. V. Nagarajan, R. Chandiramouli, Appl. Surf. Sci. 344 (2015) 65-78.
9. Q. Yin, T. Shen, J. Li, C. Ning, Y. Xue, G. Chen, M. Xu, F. Wang, Y.-F. Song, Y. Zhao, X. Duan, Chem. Eng. J. 470 (2023) 144416.
10. J. Li, L. Dong, L. Xiong, Y. Yang, Y. Du, L. Zhao, H. Wang, S. Peng, Int. J. Hydrogen. Energy 41 (2016) 12038-12048.
11. J. Li, L. Dong, L. Xiong, Y. Yang, Y. Du, L. Zhao, H. Wang, S. Peng, Int. J. Hydrogen. Energy 41 (2016) 12038-12048.
12. B. Steinhauer, M.R. Kasireddy, J. Radnik, A. Martin, Appl. Catal. A:Gen. 366 (2009) 333-341.
13. C. Fan, Y.A. Zhu, Y. Xu, Y. Zhou, X.G. Zhou, J. Chem. Phys. 137 (2012) 014703.
14. F. Menegazzo, M. Signoretto, F. Pinna, P. Canton, N. Pernicone, Appl. Catal. A: *Gen.* 439 (2012) 80-87.
15. A. Ota, E. Kunkes, J. Krohnert, M. Schmal, M. Behrens, Appl.Catal. A: Gen. 452 (2013) 203-213.
16. P.S. Moussounda, M.F. Haroun, B.M. Passi-Mabiala, P. Légaré, Surf. Sci. 594 (2005) 231-239.
17. L. Foppa, M. Iannuzzi, C. Copéret, A. Comas-Vives, J. Catal. 371 (2019) 270-275.
18. K. Li, Z. Zhou, Y. Wang, Z. Wu, Surf. Sci. 612 (2013) 63-68.
19. K. Li, M. Jiao, Y. Wang, Z. Wu Surf. Sci. 617 (2013) 149-155.
20. P. C. Psarras, D. W. Ball, Computational. and Theoretical Chem. 1063 (2015) 1-9.
21. Z. Yonghui, L. Shenggang, S. Yuhan, Chin. J. Catal. 34 (2013) 911-922.
22. H. Ahlafi, M. Nawdali, A. K. Bencheikh, D. Bianchi, Bull. Soc Chim. Belg.106 (1997) 245-262.
23. M. C. Wu, D. W. Goodman, J. Am. Chem. Soc. 116 (1994) 1364-1371.
24. M. C. Wu, D. W. Goodman, Surf. Sci. Lett. 306 (1994) L529-L533.
25. J.H. Larsen, I. Chorkendorff, Surf. Sci. 405 (1998) 62-73.
26. L. M. M. Koranne, D. W. Goodman, Methane and Alkane Conversion Chemistry; Plenum Press: New York, 1995; p 49.
27. I. M. Ciobîca, F. Frechard, R. A. van Santen, A. W. Kleyn, J. Hafner, J. Phys. Chem. B, 104 (2000) 3364-3369.
28. I. M. Ciobîca and R. A. van Santen, J. Phys. Chem. B 106 (2002) 6200-6205.
29. R. L. Arevalo, S. M. Aspera, M. C. S. Escaño, H. Nakanishi, H. Kasai, ACS Omega 2 (2017) 1295-1301.
30. J. Carey, M. Nolan, Appl. Catal. B: Environ. 197 (2016) 321-336.
31. F. He, K. Li, G. Xie, Y. Wang, M. Jiao, H. Tang, Z. Wu, Appl. Surf. Sci. 360 (2016) 826-832.
32. S.J. Yuan, L.J. Meng, J.L. Wang, J. Phys. Chem. C 117 (2013) 14796-14803.
33. A. Kokalj, N. Bonini, S. de Gironcoli, C. Sbraccia, G. Fratesi, S. Baroni, J. Am. Chem. Soc. 128 (2006) 12448-12454.
34. R. Zhang, T. Duan, L. Ling, B. Wang, Appl. Surf. Sci. 341 (2015) 100-108.
35. X. Sun, R, Zhang, B. Wang, Appl. Surf. Sci. 265 (2013) 720-730.
36. H. Zheng, R. Zhang, Z. Li, B. Wang, J. Mol. Catal. A: Chem. 404-405 (2015) 115-130.
37. L. C. Grabow and M. Mavrikakis, ACS Catal., 1 (2011) 365-384.
38. R. Zhang, G. Wang, and B. Wang, J. Catal., 305 (2013) 238-255.
39. M. Zhang, R. Yao, H. Jiang, G. Li, Y. Chen, RSC Adv. 7 (2017) 1443-1452.
40. J. R. Rostrup-Nielsen, J.H. B. Hansen, J. Catal. 144 (1993) 38-49.
41. D. Qin and J. Lapszewicz, J. Catal. Today 21 (1994) 551-560.
42. https://wiki.fysik.dtu.dk/dacapo(lastedited2010-10-2515:12:43).
43. https://wiki.fysik.dtu.dk/ase(lastupdate2016-04-1409:46:20).
44. D. Vanderbilt, Phys. Rev. B 41 (1990) 7892-7895.
45. J.P. Perdew, J.A. Chevary, S.H. Vosko, K.A. Jackson, M.R. Pederson, D.J. Singh, C. Fiolhais, Phys. Rev. B 46 (1992) 6671-6687.
46. H.J. Monkhorst, J.D. Pack, Phys. Rev. B 13 (1976) 5188-5192.
47. CRC Handbook of Chemical and Physics, vol.81, first ed. CRC Press, Boca Raton, 2000.

48. W. Lai, D. Xie, D. H. Zhang, Surf. Sci. 594 (2005) 83-92.
49. D.C. Sorescu, Phys. Rev. B 73 (2006) 155420-
50. M. F. Haroun, P.S. Moussounda, P. Légaré, Catal. Today 138 (2008) 77-83.
51. Y. Morikawa, H. Ishii, K. Seki, Phys. Rev. B 69 (2004), 041101(R)
52. B. Hammer, J.K. Nørskov, Surf. Sci. 343 (1995) 211-220.
53. B. Hammer, Topics Catal. 37 (2006) 3-16.